Nanotechnology **18** (2007) 465504 (5pp) doi:10.1088/0957-4484/18/46/465504

Synthesis of Ba-doped CeO_2 nanowires and their application as humidity sensors

Zuwei Zhang[1], Chenguo Hu[1,4], Yufeng Xiong[2], Rusen Yang[3] and Zhong Lin Wang[3]

[1] Department of Applied Physics, Chongqing University, Chongqing 400044, People's Republic of China
[2] National Center for Nanoscience and Technology, Beijing 100080, People's Republic of China
[3] School of Materials Science and Engineering, Georgia Institute of Technology, Atlanta, GA 30332, USA

E-mail: hucg@cqu.edu.cn

Received 8 August 2007, in final form 18 September 2007
Published 12 October 2007
Online at stacks.iop.org/Nano/18/465504

Abstract
Ba-doped CeO_2 nanowires were obtained from CeO_2 particles through a facile composite-hydroxide-mediated (CHM) route. The products were characterized by x-ray diffraction (XRD), field emission scanning electron microscopy (FE-SEM), transmission electron microscopy (TEM) and high-resolution transmission electron microscope (HRTEM). The formation process of the product was discussed. Humidity sensors based on the source material CeO_2 particles, Ba-doped CeO_2 nanowires grown for 12 and 72 h, were fabricated. The responses to humidity for static and dynamic testing proved that both doping Ba into CeO_2 and converting morphology into a nanowire can improve the humidity sensitivity. The resistance changes from 465 to 3.9 MΩ as the relative humidity (RH) increases from 25% to 88%, indicating promising applications of Ba-doped CeO_2 nanowires in environmental monitoring.

(Some figures in this article are in colour only in the electronic version)

1. Introduction

Nanowires have been attracting great research interest in the last several years. They have been demonstrated to exhibit superior electrical, optical, mechanical and thermal properties, and can be used as fundamental building blocks for nano-scale science and technology, ranging from chemical and biological sensors, field effect transistors to logic circuits [1–7]. Recently, nanowire paper with the function of write-erase-rewrite, made from TiO_2 nanowires, has been produced [8]. Although the methods of synthesizing nanomaterials are diverse, a facile, controllable and low-cost route to prepare nanowires is still a challenge.

The materials for humidity sensors are generally organic polymers or metal oxides. Humidity sensors based on organic polymers have many challenges due to their weak mechanical strength and poor physical and chemical stability. Ceramic types of humidity sensors are superior in performance to the polymeric type, because of their high stability towards a variety of chemical species, a wide range of operating temperatures, and fast response to the changes in humidity. Recent investigations have presented that humidity sensors based on CeO_2 powder show poor sensitivity [9], but that a humidity sensor based on CeO_2 nanowires has shown a fast response [10].

In this paper, to explore the properties of a metal-doped CeO_2 nanowire, first we synthesize Ba-doped nanowires using the CHM approach, which is an effective new approach for synthesizing oxide nanostructures [11–15]. The method is based on the reaction of source materials in a solvent of eutectic composite-hydroxides at a temperature of ∼200 °C and atmosphere pressure without using an organic dispersant or capping agent. This methodology provides a one-step, convenient, low-cost, nontoxic and mass-production route for the synthesis of nanostructured functional materials. The as-

[4] Author to whom any correspondence should be addressed.

produced nanocrystals have a clean surface, which is most favorable for further investigating its intrinsic properties and greatly improving its function [12, 15, 16], as well as for modifying its surface in bio applications. Second, humidity sensors based on source CeO_2 particles, Ba-doped CeO_2 nanowires grown for 12 and 72 h, are fabricated and the humidity sensitivity is investigated.

2. Experimental details

The Ba-doped CeO_2 is synthesized through the newly invented nanomaterial fabrication route of the CHM method [11–15]. In a typical reaction, a 9 g amount of mixed NaOH and KOH with a Na/K ratio of 51.5:48.5 is placed in a 25 ml covered Teflon vessel. A mixture of 1 m mol CeO_2 and 1 m mol $BaCO_3$ is added into the vessel as the raw materials for the reaction. Then, the vessel is put in a furnace pre-heated to 200 °C. After the hydroxides are completely molten, the molten reactants are mixed uniformly by shaking the vessel. After reacting for 24–72 h, the vessel is taken out and cooled down to room temperature. The solid product from the reaction is dissolved in deionized water, filtered and washed first by deionized water and then by dilute acid to remove the hydroxide on its surface.

An x-ray diffractometer and energy dispersive x-ray spectroscopy (EDS) are used to investigate its crystalline phase and chemical composition. FE-SEM (Hitachi S-4800) and HRTEM (Hitachi HF-2000) are used to characterize the morphology and the size of the synthesized samples.

The thin films for humidity sensitivity sensors are prepared from source CeO_2 particles, Ba-doped CeO_2 nanowires grown for 12 h and 72 h, respectively. The samples are first dispersed in ethanol, and then dropped on top of pre-deposited Au electrodes on the surface of a Si wafer. The dimensions of the film are 5 mm in length, 3 mm in width, and ~20 μm in thickness. Ohmic contacts for the planar film with copper wires are made by silver paste. The measurements are carried out by putting the sensors in an airproof glass vessel with a volume of 2 l. A hygroscope is placed into the vessel to monitor the relative humidity during the experiment process. The sensor's resistance is measured by an external testing circuit.

3. Result and discussion

Figure 1(a) shows the XRD pattern of the source material CeO_2 (curve 1) and as-synthesized products grown for 12 h (curve 2), 48 h (curve 3), and 72 h (curve 4). All peaks of the source material CeO_2 (curve 1) can be indexed as the pure cubic phase ($Fm\bar{3}m$, JCPDS 34-0394) with a lattice constant $a = 0.5411$ nm. It can be seen clearly that, besides the peaks belonging to CeO_2 structure, there are some peaks marked in dots belonging to the $BaCO_3$ structure in the spectra of the product grown for 12 h (curve 2). These peaks of the $BaCO_3$ structure are weakened as the growth time increases (curve 3), and at last disappear for the product in the 72 h growth (curve 4), indicating a pure CaF_2 structure. The lattice constant of the CeO_2 will be expanded when it is doped with Ba. Such an expansion can be detected by XRD measurement because the lattice expansion deduces that diffraction peaks shift toward smaller angles. To explore this point, we compare the 111

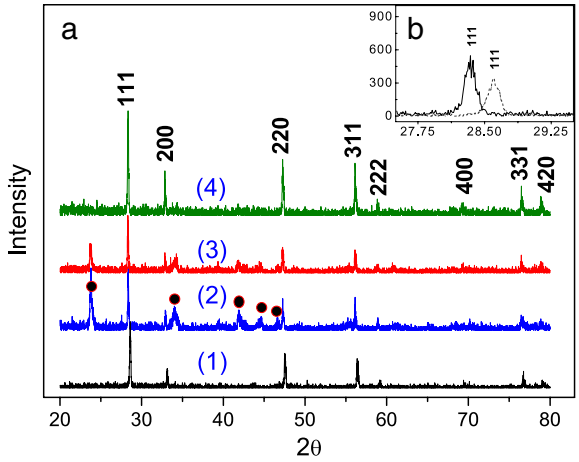

Figure 1. (a) XRD patterns of source material CeO_2 (curve 1) and as-synthesized products grown for 12 h (curve 2), 48 h (curve 3) and 72 h (cure 4). (b) Detailed XRD 111 peak of source material CeO_2 and as-synthesized products grown for 72 h. $BaCO_3$ (•).

peak of the Ba-doped CeO_2 sample (solid line) with a source material CeO_2 (dot line), as shown in figure 1(b). It can easily be found out that there is a small difference in the 111 peak locations for the Ba-doped CeO_2 sample and the source material CeO_2, where the former is at 28.34° but the latter is at 28.61°, as is shown in figure 1(b).

Figure 2 shows the typical FE-SEM images of the source material CeO_2 (a), and the Ba-doped CeO_2 sample grown for 12 h (b), 48 h (c), and 72 h (d). The particle morphology of the source material CeO_2 with the diameter ranging from 500 nm to 2 μm can be seen. When doped with Ba, the particles convert gradually into nanowires, as shown in figures 2(b)–(d). The lengths of the nanowires increase with increasing growing time. Accompanying many anomalous products, only a small number of nanowires forms during the initial 12 h growth. Almost all of the products turned into nanowires with a length of 3–10 μm after 48 h of growth, except for a few anomalous products. As the growth time is prolonged to 72 h, the length of the nanowires reaches 6–20 μm without any anomalous particles. Figure 3 exhibits the TEM images (a), the electron diffraction pattern (b) and the HRTEM images ((c), (d)) of the nanowires for a 48 h growth. The electron diffraction pattern of the selected area marked in figure 3(a) is shown in figure 3(b), indicating that the nanowire is a single crystal. The HRTEM images, as shown in figures 3(c) and (d), exhibit the single-crystal structure of the nanowire, and there is no contamination on its surface. The electron diffraction pattern, as well as the HRTEM, implies that the nanowire has the (2 2 0) plane as its growth front. The EDS is taken for a single Ba-doped CeO_2 nanowire in figure 3(e), indicating the existence of Ce, Ba, and O in the nanowire, while the Cu and C come from the TEM grid.

The interesting morphological conversion of the CeO_2 from anomalous particles into single-crystal nanowires might be explained by a dissolution–recrystallization mechanism [17]. The crystal growth experiences first the CeO_2 and $BaCO_3$ dissolving in the molten composite alkali solvent, and then CeO_2 recrystallizing while some Ba ions dope in, and finally crystal growth into a nanowire. This dissolution and

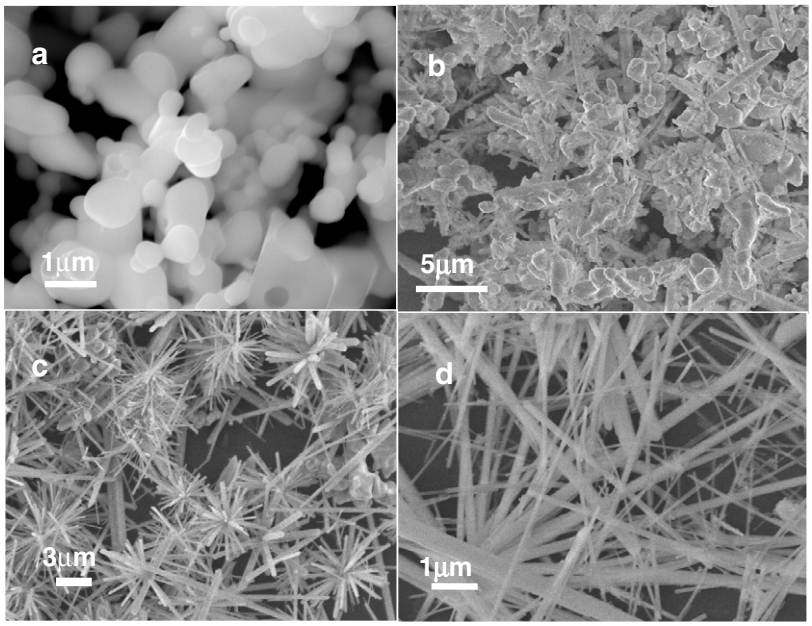

Figure 2. Typical FE-SEM images of the source material CeO_2 (a), and the Ba-doped CeO_2 sample grown for 12 h (b), 48 h (c) and 72 h (d).

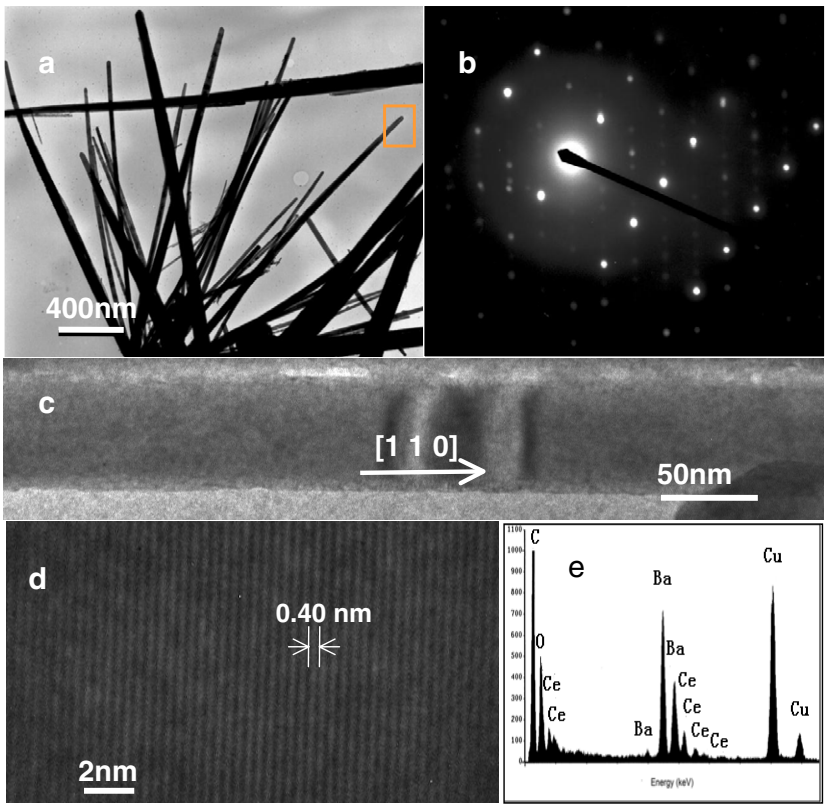

Figure 3. Typical TEM (a), electron diffraction pattern (b), HRTEM (c), (d) and EDS (e) characterizations of as-synthesized Ba-doped CeO_2 sample grown for 48 h.

recrystallization process is mainly related to temperature and growth time. In figure 2(b) we can see the CeO_2 and $BaCO_3$ dissolution and some short rods forming in the initial 12 h growth. So we presume that dissolution and recrystallization proceed gradually and end in a lack of the reactants.

The humidity sensitivity experiments are performed with humidity sensor devices made from the source material CeO_2, Ba-doped CeO_2 samples grown for 12 and 72 h, as shown in figure 4(a), while the experimental setup is shown in figure 4(b). The humidity in the vessel is controlled by mixing

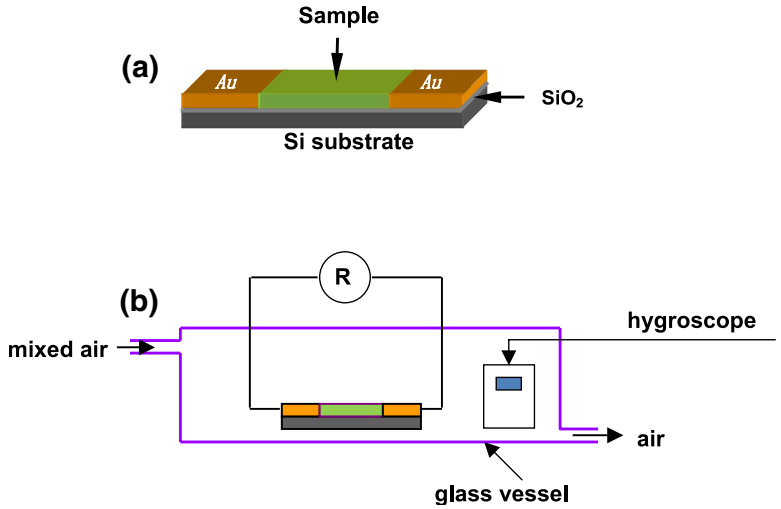

Figure 4. Schematic sketches of sensor device (a), and humidity experiment setup (b).

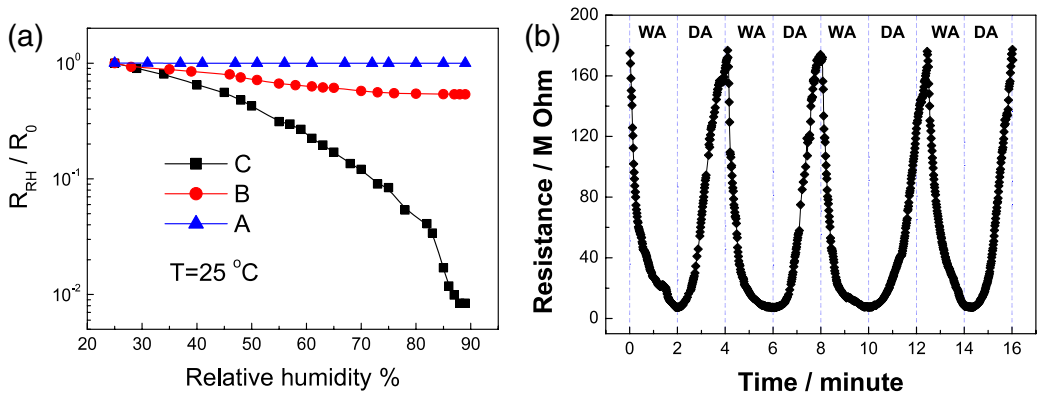

Figure 5. (a) Static response of the device made of source material CeO_2 (A), and Ba-doped CeO_2 nanowires grown for 12 h (B) and 72 h (C) to humidity. (b) Dynamic response of the Ba-doped CeO_2 grown for 72 h to humidity.

the dry air and the wet air. The relative resistances (R_{RH}/R_0) of the devices versus relative humidity (RH) are shown in figure 5(a), where R_{RH} and R_0 denote the resistance of the sensors in different humidity environments and in a humidity of 25%, respectively. Plots A, B and C in figure 5(a) represent the R_{RH}/R_0 response to RH for the devices of the source CeO_2 (A), and Ba-doped CeO_2 nanowires grown for 12 h (B) and 72 h (C) in static air of 25–90% RH at 25 °C respectively. It can clearly be seen that the resistance of the device made of the source material CeO_2 changes little with the humidity increase, while the resistance of the devices made of Ba-doped CeO_2 nanowires grown for 12 and 72 h both decrease with the increase of RH. The resistance of the device made of the 72 h sample decreases much more rapidly, and the resistance of the device in 25% RH is 465 MΩ, which is 119 times that (3.9 MΩ) in 88% RH. The static testing results indicate that both doping Ba into CeO_2 and converting the morphology into a nanowire can improve the humidity sensitivity.

Furthermore, to prove some important parameters for a sensor device (response time, recovery time, and reproducibility), dynamic testing of the device in a certain RH is performed in figure 5(b), in which we call dry air DA and wet air WA for short. The device is put in the vessel with an initial RH of 55% and an initial resistance of about 175 MΩ. When wet air of about 85% RH is switched into the vessel, the resistance of the device decreases rapidly. After 2 min, the resistance of the device is reduced to 8 MΩ and then changed slowly. Then dry air of about 25% RH is switched into the vessel and the resistance recovered to about 175 MΩ in 2 min. At the same time, another three circles follow after the previous one, proving good reproducibility of the sensitivity.

A few mechanisms have been proposed to explain the surface conductivity change in the presence of water vapor [18–20]. In general, it experiences first the chemisorbing of monolayer water with proton transfer among hydronium (H_3O^+), where the electrical response depends on the number of water molecules adsorbed on the sensor surface; and then the physisorbing of multilayer water with increasing humidity, where H_3O^+ appears in the physisorbed water and serves as a charge carrier. H^+ ions can move freely in the physisorbed water according to Grotthuss's chain reaction [21–23]. Electrolytic conduction takes the place

of protonic conduction at high humidity. This is further confirmed from the characteristics of the resistance versus relative humidity of the sensor in figure 5(a). The resistance decreases nonlinearly with increasing humidity, implying ion-type conductivity as the humidity-sensing mechanism [24–26]. From figure 5(b), we can see that the response speed is faster than the recovery speed. This may contribute to the thickness of $\sim$20 μm (from a side view of the SEM). The resistance drops rapidly at several layers of adsorption water on the surface at first tens of seconds and then reduces slowly, as a film of such a thickness can be regarded as a parallel connection of two resistances, one with small resistance (up layer) and another with a big resistance (deep layer). The current on the film prefers to go through the small resistance. So the resistance reaches steady state quickly. However, the situation for the recovery process is just reversed. The resistance increases with desorption of water molecules, but it is difficult to desorb the water molecules in the deep layers. We presume that the thinner the film, the less that the recovery time should be.

Doping Ba^{+} into CeO_2 leads to higher charge density in the surface. In this case, a strong electric field is induced around the surface of Ba-doped CeO_2. This strong electric field augments the ionization of water molecules and further affects the deeper physisorbed water [10]. On the other hand, the large surface-to-volume ratio of the nanowires plays an important role in their conduction. The large communicating interspaces due to the network-like nanowire films and the higher pressure on a convex surface of the nanowires probably contribute to the fast response and rapid recovery of the humidity sensors [10].

4. Conclusions

In summary, Ba-doped CeO_2 nanowires can be obtained from CeO_2 particles through the CHM approach. The morphology conversion of the products could be explained by a dissolution–recrystallization mechanism. Test results for humidity sensitivity based on source CeO_2 particles, and Ba-doped CeO_2 nanowires grown for 12 and 72 h indicate that both doping Ba into CeO_2 and converting the morphology into a nanowire can improve the humidity sensitivity. Considering the excellent chemical and thermal stability, Ba-doped CeO_2 nanowires could be a potential material for humidity detecting applications.

Acknowledgments

This work is funded by the National Natural Science Foundation of China (NSFC) (90406024), the Natural Science Foundation Project of Chongqing Science and Technology (NSF Project of CSTC) (2006BB4241) and Chongqing University Postgraduates' Science and Innovation fund (200701Y1A0210207).

References

[1] Wang Z L (ed) 2003 *Nanowires and Nanobelts* vol 1–2 (Boston, MA: Kluwer–Academic)
[2] Yang C, Zhong Z and Lieber C M 2005 *Science* **310** 1304
[3] Lieber C M and Wang Z L 2007 *MRS Bull.* **32** 99
[4] Wang X D, Song J H, Liu J and Wang Z L 2007 *Science* **316** 102
[5] Wang Z L and Song J H 2006 *Science* **312** 242
[6] Wu Y, Xiang J, Yang C, Lu W and Lieber C M 2004 *Nature* **430** 61
[7] He R and Yang P 2006 *Nat. Nanotechnol.* **1** 42
[8] Dong W J, Cogbill A, Zhang T R, Ghosh S and Tian Z R 2006 *J. Phys. Chem.* B **110** 16819
[9] Parvatikar N, Jain S, Bhoraskar S V and Ambika Prasad M V N 2006 *J. Appl. Polym. Sci.* **102** 5533
[10] Fu X Q, Wang C, Yu H C, Wang Y G and Wang T H 2007 *Nanotechnology* **18** 145503
[11] Liu H, Hu C G and Wang Z L 2006 *Nano Lett.* **6** 1535
[12] Hu C G, Liu H, Lao C S, Zhang L Y, Davidovic D and Wang Z L 2006 *J. Phys. Chem.* B **110** 14050
[13] Hu C G, Zhang Z W, Liu H, Gao P X and Wang Z L 2006 *Nanotechnology* **17** 5983
[14] Miao J, Hu C G, Liu H, Xiong Y F and Feng B 2007 *Mater. Lett.* doi:10.1016/j.matlet.2007.05.009
[15] Hu C G, Liu H, Dong W T, Zhang Y Y, Bao G, Lao C S and Wang Z L 2007 *Adv. Mater.* **19** 470
[16] Wang N, Hu C G, Xia C H, Feng B, Zhang Z W, Xi Y and Xiong Y F 2007 *Appl. Phys. Lett.* **90** 163111
[17] Lu J, Xie Y, Xu F and Zhu L Y 2002 *J. Mater. Chem.* **12** 2755
[18] Chou K S, Lee T K and Liu F J 1999 *Sensors Actuators* B **56** 106
[19] Zhao J, Bulduml A, Han J and Lu J P 2002 *Nanotechnology* **13** 195
[20] Chen Z and Lu C 2005 *Sensor Lett.* **3** 274
[21] Qu W M and Meaa J U 1997 *Sci. Technol.* **8** 593
Sears W M 2000 *Sensors Actuators* B **67** 161
[22] Anderson J H and Parks G A 1968 *J. Phys. Chem.* **72** 3362
[23] Pokhrel S and Nagaraja K S 2003 *Sensors Actuators* B **92** 144
[24] Traversa E 1995 *Sensors Actuators* B **23** 135
[25] Kulwicki B M 1984 *J. Phys. Chem. Solids* **45** 1015
[26] Lee C Y and Lee G B 2005 *Sensor Lett.* **3** 1